Vol. 597: 47–64, 2018
https://doi.org/10.3354/meps12599

MARINE ECOLOGY PROGRESS SERIES
Mar Ecol Prog Ser

Published June 11

Composition and functional diversity of macrofaunal assemblages on vertical walls of a deep northeast Pacific fjord

Ryan Gasbarro[1,*], Di Wan[1,2], Verena Tunnicliffe[1,3]

[1]School of Earth and Ocean Sciences, University of Victoria, Victoria, BC V8W 2Y2, Canada
[2]Institute of Ocean Sciences, Fisheries and Oceans Canada, Sidney, BC V8L 5T5, Canada
[3]Department of Biology, University of Victoria, Victoria, BC V8W 2Y2, Canada

ABSTRACT: Fjords are temperate zone coastal features with strong horizontal and vertical environmental gradients, but the composition and function of biota living on the confining walls are poorly documented due to relative inaccessibility. We present results from remotely operated vehicle imagery of the subphotic (50 to 680 m depth) bedrock walls from 3 sites in Douglas Channel, a northeast Pacific fjord complex. We assessed the composition and abundance of the wall fauna and correlated these data with the water mass flux character of the fjord. Using a suite of morphological traits, we also identified areas of high function through habitat formation. This baseline record of hard substratum benthos in Douglas Channel revealed diverse assemblages marked by vertical zonation, dense animal cover (≥80% areal cover in some areas), and some variation from fjord head to mouth. The deepest portions of the fjord at our most seaward site (≥400 m) harbored the most taxonomically and functionally rich assemblages, with multiple species exclusive to this zone; there was a sharp increase in animal cover in shallow (≤150 m) areas caused by the appearance of dictyonine glass sponges and increases in articulate brachiopod, zoanthid, and encrusting sponge cover. Animal cover was positively correlated with winter kinetic energy density fluxes, indicating that a consistent oceanic influx augments biomass above 150 m most likely by increasing particle delivery rates. Our findings demonstrate that fjord walls support high biomass, high functioning, diverse, and expansive biosystems that warrant further study and consideration when developing coastal ocean management plans.

KEY WORDS: Epibenthos · Suspension feeders · Functional traits · Habitat formation · Flux · Douglas Channel

INTRODUCTION

Fjords are features of mid to high latitudes, formed after the last glaciation, which created coastal incisions up to 100s of km in length. As such, they serve as conduits for organisms that normally inhabit offshore regions to venture close to land, such as deep-water fish (Boje et al. 2014) and mammals (Keen et al. 2017). They provide the only close contact humans on land have with ocean depths that can reach 1000 m. In addition, these waterways can allow passage for large vessels (e.g. tankers, cargo ships) to access secure inland ports. Fjordic walls often feature hard substrata where steep topography and low sediment loading facilitate settlement of sessile organisms. Deep fjordic areas below the photic zone (i.e. >~50 m depth) are relatively inaccessible without guided camera systems or submersibles. For this reason, deep vertical bedrock substrata remain a poorly studied ecosystem, with most studies providing only qualitative descriptions of the biota (Wahl 2009).

*Corresponding author: rgasbarr@uvic.ca

In shallow (<50 m) systems, vertical bedrock is dominated by a diverse suspension-feeding fauna structured by larval recruitment (Smith & Witman 1999) and water column properties (e.g. ambient flow) that influence the delivery rate (Leichter & Witman 1997) and concentration (Lesser et al. 1994) of particulate organics. Where physical conditions permit, bedrock substrata are densely covered, and space competition becomes the dominant force shaping the diversity of the sessile fauna (Buss 1990). Miller & Etter (2011) showed that the abundance and diversity of organisms on vertical rock surfaces was higher than on adjacent horizontal surfaces in the subtidal Gulf of Maine; this pattern was largely driven by intense competition for space between sessile invertebrates and phototrophs.

Similar processes influence subphotic hard substratum assemblages. Genin et al. (1992) described high sponge and gorgonian cover on an abyssal rock cliff where local particle fluxes in a boundary current were enhanced. Submarine canyon walls provide refuge from deep-sea anthropogenic disturbances such as bottom trawling, and downslope carbon transport and internal water fluxes can support dense suspension-feeding communities absent from adjacent slopes (Huvenne et al. 2011). Similarly, some seamounts possess high biomass relative to adjacent bottoms, with a great proportion owing to increases in sessile filter-feeding invertebrates and their predators (Rowden et al. 2010). Haedrich & Gagnon (1991) also found a rich community of suspension-feeding fauna covering deep rocky outcrops in a Newfoundland fjord, while muddy slopes and the fjord bottom were sparsely colonized.

The west coast of North America has more fjords than any other fjord province on the planet (Syvitski et al. 1987), and studies here account for much of the work done on deep fjord epilithos (e.g. Levings et al. 1983). The fjordic environment can change spatially with terrestrial inputs at the landward head and oceanic inputs at the mouth, creating steep horizontal gradients in variables such as salinity (Pickard 1961), sediment loading (Carney et al. 1999), larval supply (Quijon & Snelgrove 2005), and succession following disturbance (Moon et al. 2015) over relatively short distances. High productivity and associated sinking particle fluxes create steep gradients with depth in variables such as dissolved oxygen (Anderson & Devol 1973) and pH (Jantzen et al. 2013). Northeast Pacific fjords harbor large expanses of vertical bedrock substrata with unusual and often dense assemblages along these gradients (Tunnicliffe 1981, Farrow et al. 1983).

The Douglas Channel complex incises the coast of northern British Columbia, Canada, for about 95 km with depths to nearly 700 m. The presence of a port at Kitimat and open ocean access have attracted proposals to develop a diluted bitumen pipeline terminus and several liquid natural gas facilities (Enbridge 2010, Hughes 2015). These projects would result in a sharp increase in tanker traffic, and thus the chance of a hydrocarbon spill that could have long-lasting deleterious effects on the local biota (Webster et al. 1997, Dew et al. 2015). However, there is little information on benthic community structure or function to assess vulnerability to human-induced stressors, especially for species such as sponges and corals. Douglas Channel has an estuarine-driven circulation with both intermediate depth inflow to compensate the surface outflow and annual deep renewal that may be modified by the presence of 2 sills (Macdonald et al. 1983). Water mass behaviour that brings both land-based organics and outer coast nutrient inputs (Johannessen et al. 2015) is likely to affect the nature and distribution of benthic organisms, particularly those directly exposed to fluids on the fjord walls. Spring melt outflows deliver more particulates to the upper fjord while a mid-depth wedge of shelf water enters at the mouth.

We undertook 9 remotely operated vehicle (ROV) imaging transects from 3 sites in Douglas Channel. Our first objective was to examine the subphotic animal assemblages on the fjord walls to determine the distribution, abundance, and diversity of macrofauna with depth and location in the fjord, and correlate these results with water properties. We tested the hypothesis that the abundance and diversity of suspension-feeders on the fjord walls reflect the vertical structure of water movement in the fjord, using current records from year-long deployments of 2 profiling moorings in the inlet. We also assessed the distribution of unique biological effect traits (Naeem & Wright 2003) in the assemblages as a proxy for functional richness (Keyel & Wiegand 2016); we chose traits related to body morphology, and thus to biogenic habitat formation, to identify areas of high ecological function (Hooper et al. 2005). This study provides baseline information about the deep biota in a fjord that may see rapid increases in large ship transits.

MATERIALS AND METHODS

Study site

Douglas Channel is part of a fjord complex on the northern coast of British Columbia, Canada, extend-

ing about 95 km from the upper estuary to Hecate Strait (Fig. 1). Two sills approximately 200 m deep define a northern basin (to 400 m depth) and a southern basin reaching 680 m in Squally Channel. The depth ranges at our sites were 50 to 320 m at Maitland Island, 50 to 420 m at McKay Reach, and 170 to 680 m at Squally Reach.

Circulation in the fjord is driven primarily by wind forces and freshwater input from the Kitimat and Kemano rivers and scattered streams. The surface freshwater discharge peaks in May due to snowmelt and again in autumn/winter due to rain (Macdonald et al. 1983). This estuarine surface outflow is balanced by the compensating inflow immediately below the surface from Hecate Strait, where the shallow bank constrains the intrusion to intermediate depth of 70 to 150 m (Wan et al. 2017). The incoming intermediate water from the continental shelf is storm-mixed in autumn and winter, importing nutrients into the fjord system that otherwise generates little *in situ.* Johannessen et al. (2015) described strong connections in water properties of this layer between the Strait and the fjord throughout the year. An additional nutrient influx comes when wind-driven upwelling onto the Hecate Strait shelf drives annual deep-water renewal in the fjord. Starting from mid-May to early June, dense shelf water intrudes under the bottom water of Douglas Channel over 3 mo (Wan et al. 2017). After renewal, the temperature profiles are uniform below ~100 m, and oxygen concentrations in the deep basins increase by ~1 to ~3.5 ml l^{-1} (Johannessen et al. 2015). The physical and chemical dynamics of Douglas Channel appear to be predictable over decadal time scales (Macdonald et al. 1983, Wright et al. 2016).

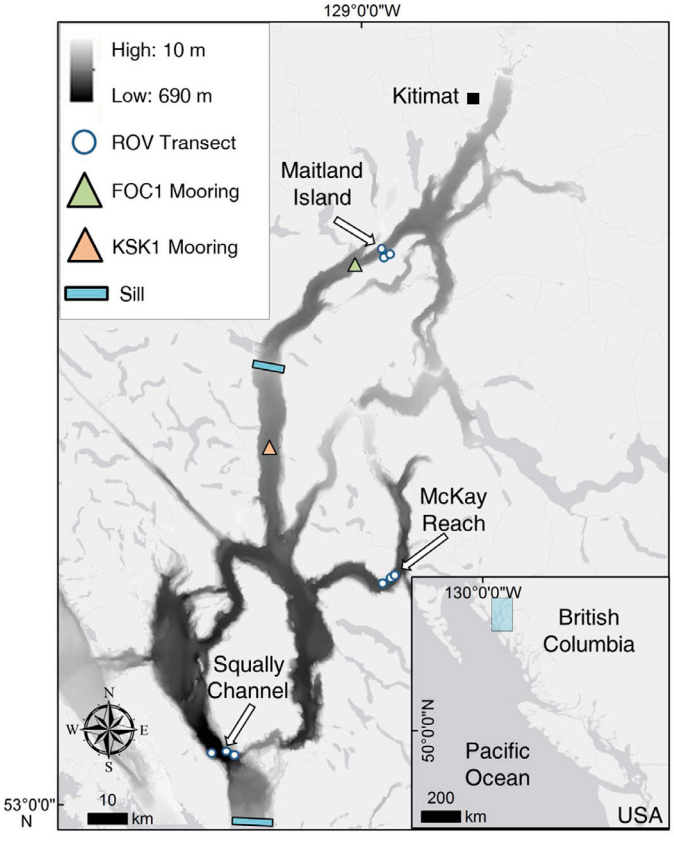

Fig. 1. Distribution of ROV transects in the Douglas Channel fjord complex and geographic setting of the fjord (inset). Multi-beam bathymetry data are at 10 m grid cell resolution. Three dives were executed at each of 3 labeled sites starting on the bottom and ascending near-vertical walls. Locations of the 2 moorings with acoustic Doppler current profilers (FOC1 and KSK1) are indicated. The northern sill is 200 m and the southern 140 m depth

Bedrock formations in Douglas Channel are metamorphic granitoids with gneissic diorite around Maitland and quartz monzonite and diorites in the McKay and Squally sections (Roddick 1970). Fjord structure and wall erosion formed by ice movement during Wisconsonian glaciation; ice retreat, then sea inundation, occurred after 13 000 BP (Clague 1985). As with all of the northeast Pacific coast, the deep fjord communities are post-glacial invasions.

Kinetic energy flux

Kinetic energy flux per unit volume ($uE = 1/2\ \rho \times u^3$, where u is the velocity and ρ is the water density; Kundu & Cohen 2008) can be used as a measure of the transport of the kinetic energy across a surface by integrating it over a unit area to obtain the kinetic energy flux density ($\sum uE\Delta a = uEA$, where A is the unit area). The cubic velocity term (u^3) in kinetic energy flux density represents turbulence, and thus is relevant to passive suspension-feeding organisms on the wall; particle encounter frequency increases unimodally with turbulence until drag forces at high current velocities impair the function of feeding appendages (Hart & Finelli 1999). We calculated the kinetic energy flux density (kg m^2 s^{-3}) from along-channel currents measured with acoustic Doppler current profilers (ADCPs) and current meters during the July 2014–2015 deployment at FOC1 and KSK1 (Fig. 1). The FOC1 mooring was chosen due to its close proximity to the Maitland Island site. KSK1, while located in a neighboring channel, has similar water properties and appears well connected to McKay Reach (D. Wan unpubl. data).

At FOC1, there were single point current meters at 53 and 200 m, an upward-looking ADCP at 39 m

(300 kHz, 4 m bin size), and a downward-looking ADCP at 100 m above the bottom (300 kHz, 4 m bin size). At KSK1, there was a single point current meter at 150 m, and upward-looking ADCPs at 40 m depth (300 kHz, 2 m bin size) and at 11 m from the bottom (75 kHz, 16 m bin size). Summer values were calculated from May to September during which the basins underwent deep-water renewal processes, and winter values were calculated from the non-renewal months of October to April.

Wall transects

We selected 3 sites in areas where bathymetry indicated the likely presence of steep to vertical slopes with bare bedrock. In late September 2015, we executed 3 transects at each of the Maitland Island, McKay Reach, and Squally Reach sites (Fig. 1). These 9 slow vertical ascents conducted with the ROV 'ROPOS' formed our transects up the walls. High definition (HD) video, CTD (SBE 19plus V2; Sea-Bird Electronics) and oxygen probe (SBE43; Sea-Bird Electronics) data were recorded for each transect. The CTD and oxygen sensors were both mounted on the front of the ROV that maintained a distance of about 1 m from the wall. We collected navigation data on a per second basis using the ROV's internal high-precision ultra-short baseline system. The ROV ascended at ~0.1 to 0.3 knots (about 10 cm s^{-1}) while imaging the wall surface with a forward-mounted HD 1080i video camera; field of view was 1 to 2 m across measured by a pair of parallel horizontal lasers calibrated at 10 cm apart. A 12.1 megapixel Nikon D7000 digital camera captured high resolution photographs. Transects ended at about 40 m depth at Maitland and McKay, and at 175 m at Squally Reach where no cliffs occurred above this depth.

Video and image analyses

Image analysis incorporated 2 stages: (1) initial full video scan to characterize the entire wall surface encountered and to generate estimates of faunal cover; and (2) detailed still frame analysis of overlaid quadrats on vertical walls. First, video transects were annotated using VideoMiner v.2.1.2.0 (custom Fisheries and Oceans Canada video annotation software) that creates a second-to-second database of continuous features observer-adjusted as they change. We then retrieved (1) percent cover estimates for the dominant substrata (sediment, bedrock, shell hash, and dead sponge), and vertical relief (i.e. estimated slope), and (2) estimates of the percentage of substratum occupied by organisms. Every 10 s, we noted the presence of major taxonomic groups. Over the 9 transects, the database comprised over 78 000 non-overlapping records of substratum and biological observations, along with CTD data synchronized by timestamp (see Table S1 in the Supplement at www.int-res.com/articles/suppl/m597p047_supp.pdf). Kinetic energy flux density values were generated in 1 m increments by spline interpolation between data points separated by 16 m; these 1 m values were then averaged into 10 m depth bands. Kinetic energy flux values and faunal cover estimates per 10 m depth band were related via linear regressions.

For the second stage of analysis, we queried portions of the video with slope >45° to isolate segments with vertical or near-vertical walls, low to moderate sediment drape, and bedrock as the primary substratum. Video framegrabs (n = 5 or 6) in each 25 m depth band from the bottom up to 50 m provided the basis for a quadrat analysis using PhotoQuad software (Trygonis & Sini 2012); quadrat locations were randomly selected by timestamp with a minimum of 1 min between quadrats in order to reduce autocorrelation in adjacent quadrats. A grid of numbers from 1 to 100 was overlain on the framegrab; a 1 m^2 quadrat, overlain on the framegrab, was centered on a randomly chosen number or aligned with the nearest edge when the number was <50 cm from the image border. All animals >0.5 cm were measured for size and identified to the lowest possible taxonomic resolution using image matching with published and in-house guides plus past collections. Where possible, our identifications were verified using higher-quality digital photographs. In several cases, local experts corroborated our tentative identifications. Table 1 notes where species level was not possible and where 2 species were similar in appearance. We did not include hyperbenthic organisms (e.g. teleost fishes) if they were out of frame in the 5 s of video prior to, or after, the framegrab. This approach excluded passing organisms attracted to the ROV lights (e.g. halibut), but included non-ephemeral mobile species (e.g. rockfish). We also excluded serpulid (Annelida) tubeworms, despite their near-ubiquity, from the quadrat analysis because it was not possible to confirm that the calcareous tubes contained living animals. Autocorrelation of quadrats within transects was deemed negligible by visual inspection of ordination plots prior to analyses. Overall, this image analysis comprised 236 quadrats across the depth ranges of the 3 sampled sites.

Diversity analyses from quadrats

A 'per depth band' species-abundance matrix was created from animal identifications and counts from still frames. Then, we calculated species richness and taxonomic distinctness using 2 indices of Clarke & Warwick (2001) using the R package 'vegan' (Oksanen et al. 2017); the first taxonomic distinctness index (sΔ+) incorporated species abundances during calculation while the other strictly used species presences (Δ+).

Species count data from quadrat sampling were also analysed using the multivariate statistical software package PRIMER 6 (Clarke & Gorley 2006) with PERMANOVA (Anderson et al. 2008) in order to identify distinct assemblages by depth and location. Raw count data were square-root transformed prior to analysis to account for the contribution of low-abundance taxa to assemblage structure without eliminating the signal from abundant species. Assemblages in the data were identified by hierarchical cluster analysis (CLUSTER) on the quadrat resemblance matrix with a similarity profile (SIMPROF) test (at $p = 0.05$). The percentage similarity (SIMPER) routine was employed to determine the taxa contributing to the differences between each SIMPROF assemblage. In order to determine species contributions at the site level, we ran a SIMPER analysis for each site using count data; to reduce noise and include a larger species complement in each pairwise comparison, counts were binned into 25 m depth bands for the site analysis. We visualized patterns in the grouping of samples by site and by SIMPROF-determined assemblage in 2 dimensions using canonical analysis of principal coordinates (CAP) plots.

A permutational multivariate analysis of variance (PERMANOVA) described the variability in assemblage structure between sites. Before the PERMANOVA, a distance-based homogeneity of multivariate dispersions (PERMDISP; 999 permutations) test was employed to test for significant dispersion in the data

Table 1. Species (n = 54) observed in Douglas Channel imagery and their broad taxonomic designation; designated groups include serpulids (SP), asteroids (AS), echinoids (EC), decapods (DE), non-hexactinellid sponges (OS), actinarians (AC), gastropods (GA), cup corals (CC), bubblegum corals (BC), ophiuroids (OP), crinoids (CR), articulate brachiopods (AB), lyssacine glass sponges (LHx), dictyonine glass sponges (DHx), inarticulate brachiopods (IB), zoanthids (ZO), and rockfish (RF). Asterisks denote tentative identifications of encrusting species that were not included in the total species tally

Phylum	Order	Species	Designation
Porifera	Clathrinida	*Clathrina* cf. *coriacea**	OS
Porifera	Clathrinida	Porifera1*	OS
Porifera	Leucosolenida	*Leucandra heathi**	OS
Porifera	Axinellida	*Auletta krautteri*	OS
Porifera	Halichondrida	*Hymeniacidon* spp.	OS
Porifera	Poecilosclerida	*Cladorhiza* spp.	OS
Porifera	Poecilosclerida	*Mycale bellabellensis*	OS
Porifera	Poecilosclerida	*Myxilla lacunosa**	OS
Porifera	Tetractinellida	*Stelletta clarella**	OS
Porifera	Tetractinellida	*Poecillastra tenuilaminaris*	OS
Porifera	Verongiida	*Hexadella* spp.*	OS
Porifera	Hexactinosida	*Aphrocallistes vastus*/ *Heterochone calyx*	DHx
Porifera	Hexactinosida	*Farrea occa*	DHx
Porifera	Lyssacinosida	*Rhabdocalyptus dawsoni*/ *Staurocalyptus dowlingi*	LHx
Porifera	Homosclerophorida	*Plakina atka*	OS
Cnidaria	Actinaria	*Cribrinopsis fernaldi*	AC
Cnidaria	Actinaria	*Stomphia didemon*	AC
Cnidaria	Actinaria	*Liponema brevicornis*	AC
Cnidaria	Alcyonacea	*Paragorgia arborea*	BC
Cnidaria	Alcyonacea	*Swiftia beringi*	
Cnidaria	Alcyonacea	*Primnoa pacifica*	
Cnidaria	Antipatharia	*Antipathes* spp.	
Cnidaria	Ceriantharia	*Pachycerianthus fimbriatus*	
Cnidaria	Scleractinia	*Caryophyllia alaskensis*	
Cnidaria	Scleractinia	*Caryophyllia arnoldi*	
Cnidaria	Trachymedusae	*Ptychogastria polaris*	
Cnidaria	Zoanthidae	*Epizoanthus scotinus*	
Annelida	Sabellida	*Protula pacifica*	SP
Annelida	Sabellida	*Serpula vermicularis*	SP
Nemertea	Unknown	Nemertean1	
Brachiopoda	Craniida	*Novocrania californica*	IB
Brachiopoda	Terebratulida	*Laqueus vancouveriensus*	AB
Arthropoda	Decapoda	*Munida quadrispina*	DE
Arthropoda	Decapoda	*Pandalus* spp.	DE
Arthropoda	Decapoda	*Metacarcinus magister*	DE
Mollusca	Vetigastropoda	*Calliostoma platinum*	GA
Mollusca	Caenogastropoda	*Fusitron oregonensis*	GA
Echinodermata	Forcipulatida	*Stylasterias forreri*	AS
Echinodermata	Forcipulatida	*Pycnopodia* spp.*	AS
Echinodermata	Paxillosida	*Leptychaster anomalus*	AS
Echinodermata	Paxillosida	*Leptychaster arcticus*	AS
Echinodermata	Paxillosida	*Ctenodiscus crispatus*	AS
Echinodermata	Paxillosida	*Gephyreaster swifti*	AS
Echinodermata	Spinulosida	*Henricia sanguinolenta*	AS
Echinodermata	Valvatida	*Ceramaster patagonicus*	AS
Echinodermata	Valvatida	*Hippasteria spinosa*	AS
Echinodermata	Valvatida	*Lophaster furcilliger*	AS
Echinodermata	Valatida	*Pteraster tesselatus*	AS
Echinodermata	Comatulida	*Florometra serratissima*	CR
Echinodermata	Echinoida	*Strongylocentrotus pallidus*	EC
Echinodermata	Echinoida	*Strongylocentrotus franciscanus*	EC
Echinodermata	Aspidochirotida	*Parastichopus leukothele*	
Echinodermata	Aspidochirotida	*Parastichopus californicus*	
Echinodermata	Dendrochirotida	*Eupentacta pseudoquinquesemita*	
Echinodermata	Ophiurida	*Ophiopholis aculeata*	OP
Chordata	Stolidobranchia	*Cnemidocarpa finmarkiensis*	
Chordata	Aplousobranchia	*Diplosoma listerianum*	
Chordata	Chimaeriformes	*Hydrolagus colliei*	
Chordata	Peuronectiformes	*Hippoglossus stenolepis*	
Chordata	Scorpaeniformes	*Sebastes babcocki*	

using the deviations from centroid method to reduce the likelihood of Type I error (Anderson 2006). The PERMANOVA, with Type III (partial) sums of squares and 999 unrestricted permutations of raw data, included site as the only factor in the design.

The degree to which environmental variables correlated with the assemblages was assessed with a distance-based linear model (DistLM) using all the quadrats in the fjord. Environmental variables were normalised and assessed for covariance; if the Pearson correlation coefficient between 2 variables was greater than 0.9, one of the variables was removed (Anderson et al. 2008). Depth, temperature, dissolved oxygen, relief, areal animal cover, and areal bedrock cover were included in the null model. Final model selection was carried out using corrected Akaike's information criteria (AIC_c) and a 999 permutation stepwise selection procedure. A distance-based redundancy analysis (dbRDA) displayed the DistLM results in 2 dimensions, with quadrats identified by their SIMPROF-determined assemblage and vectors displaying individual contributions to the total variation for each variable.

We compiled a species-trait matrix from the quadrat analysis with functional trait modalities for 6 ordinal and factor traits (Table 2). For this analysis, we chose traits based on both pragmatism—given the paucity of behavioral and life-history data for our component species—and relevance to ecosystem properties through biogenic habitat formation (Hooper et al. 2005). We analyzed our species-trait matrix in conjunction with a 'per depth band' species-abundance matrix in R (R Development Core Team 2013) using the 'FD' package (Laliberté & Legendre 2010) to calculate distance-based estimates of functional evenness (FEve; Villéger et al. 2008) and functional dispersion (FDis; Laliberté & Legendre 2010). The use of solely ordinal and factor traits precluded the calculation of functional richness using a convex-hull approach, and therefore was measured as the proportion of unique trait combinations in a given depth band over the number of unique trait combinations in the entire species pool (sUTC; Keyel & Wiegand 2016).

RESULTS

In late September 2015, temperature at our study depths (50 to 680 m) decreased from 9 to 7.5°C from 50 to ~175 m, then to fairly uniform temperatures (~7.2°C) below ~200 m at Maitland and McKay transects; temperatures at Squally were 0.5 to 1.0°C warmer (Fig. 2). Dissolved oxygen generally remained above ~2.5 ml l^{-1} at all locations. The along-channel kinetic energy flux density plots (Fig. 3) showed strong surface outflux with an underlying influx at both locations in both seasons, which correspond to previously described estuarine-driven 2-layer circulation in the channel. In winter, at both instrumented locations, the influx spanned the range from about 40 to 120 m depth while summer influx was a narrower band with a bottom inflow evident near Maitland Island.

Distribution of habitat

Substratum features varied by site in the fjord. At both Maitland Island and McKay Reach, the substratum was largely comprised of bare bedrock: 57 and 76% of the video records, respectively (Table S1 in the Supplement). At Squally Reach, sediment drape predominated in 71% of the records, largely due to the greater presence of low relief and stepped slopes. Biogenic substrata, which included shell hash composed of brachiopod/bivalve shells and glass sponge skeletons, were uncommon (<5% of records) at the Maitland and McKay sites and absent at Squally. Fauna appeared specific to the substratum type. Bare

Table 2. Functional traits scored for all species (n = 54) recorded in spaced still frame quadrats. 'Habitat provision' refers to whether a species likely provides a 3-dimensional habitat (e.g. arborescent corals) or may possibly provide a habitat (e.g. shelled species) for other organisms

Functional trait	Type	Modalities
Growth form	Factor	Determinate (prone); determinate (erect); indeterminate (mound); indeterminate (tree); indeterminate (encrusting)
Preferred substratum	Factor	Bedrock; sedimented bedrock; sediment
Motility	Factor	Sessile; sedentary; surface motile; swimming
Habitat structure	Factor	Tube; free-living; epizootic; shelled
Log_{10} body size	Ordered factor	Indexed from 0–2; log_{10} max body/colony size
Habitat provision	Ordered factor	Likely; possible; none

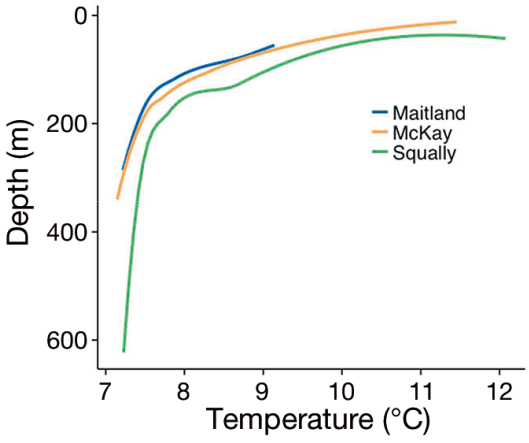

Fig. 2. Temperature profiles taken during ROV descent at each site surveyed in Douglas Channel from ROV-mounted CTDs in late September 2015. Each line is from one representative downcast, smoothed to remove noise caused by the ROV's variable descent rate. Profile shapes illustrate the steady temperature decrease from 40 to 150 m at the 2 northerly sites while Squally Reach temperatures are ca. 0.5°C warmer at comparable depths

bedrock substrata were usually densely covered and dominated by sessile species, with colonial and encrusting forms as the main space competitors. Sedimented areas were more sparsely covered, with mobile species dominating the fauna. While shell hash was nearly devoid of animals save for the occasional mobile organisms, rockfish and crustaceans were common in the 3-dimensional habitat of dead glass sponges.

Animal distributions in continuous video transects

A total of 53 taxa (>0.5 cm) from 9 phyla were seen in the continuous transects, although it was not possible to identify all to species level (Table 1). Hexactinellid sponge species are distinguished by examination of spicules; thus, dictyonines included *Aphrocallistes vastus* and *Heterochone calyx,* and lyssacines included *Rhabdocalyptus dawsoni* and *Staurocalyptus dowlingi*. The glass sponge *Farrea occa* was seen in the continuous video but not in any of the subsequent quadrats. Tubes of the serpulid annelids *Serpula vermicularis* and *Protula pacifica* were present throughout the fjord at all depths, but could not be confirmed alive or identified to the species level unless their branchial crowns were extended for feeding.

Animal assemblages on the walls ranged from scattered individuals on sediment-draped surfaces, to near 100% cover on steep walls and overhangs, to complex 3-dimensional habitats formed by hexactinellid sponges as illustrated in Fig. 4a. Differences in assemblage composition with depth and site are represented in Fig. 5 based on presence/absence of major groups. Below, we describe faunal distribution results as the data were collected; i.e. ascending from the bottom.

Serpulid worm tubes, asteroids, echinoids, decapods, non-hexactinellid sponges, and actinarians spanned the entire depth range sampled at all sites. Gastropods occurred at nearly all depths but decreased in the uppermost ~50 m of Maitland Island and McKay Reach. The comatulid crinoid *Florometra serratissima* (often associated with sponges) and cup corals of the genus *Caryophyllia* extended above 200 m in some areas, but were much more common deeper (Fig. 4e). The brittle star *Ophiopholis aculeata* was limited to water below ~300 m, and was not seen in the Maitland transects. Other taxa with a deep-water

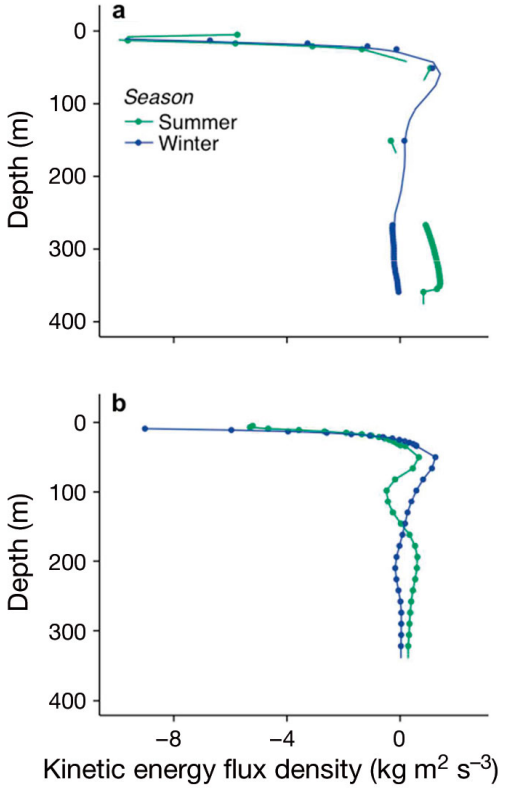

Fig. 3. Along-channel kinetic energy flux density (1/2 ρ × u^3) calculated from (a) Site FOC1 and (b) Site KSK1 acoustic Doppler current profiler moorings during July 2014 to July 2015 deployments. Points: measured values with lines connected by spline interpolation. The negative flux is in the down-fjord direction, and the positive flux is in the up-fjord direction. In the upper 150 m, the energy flux density increases and peaks at the surface (outflow) and 50 to 70 m inflow, reflecting the estuarine circulation pattern

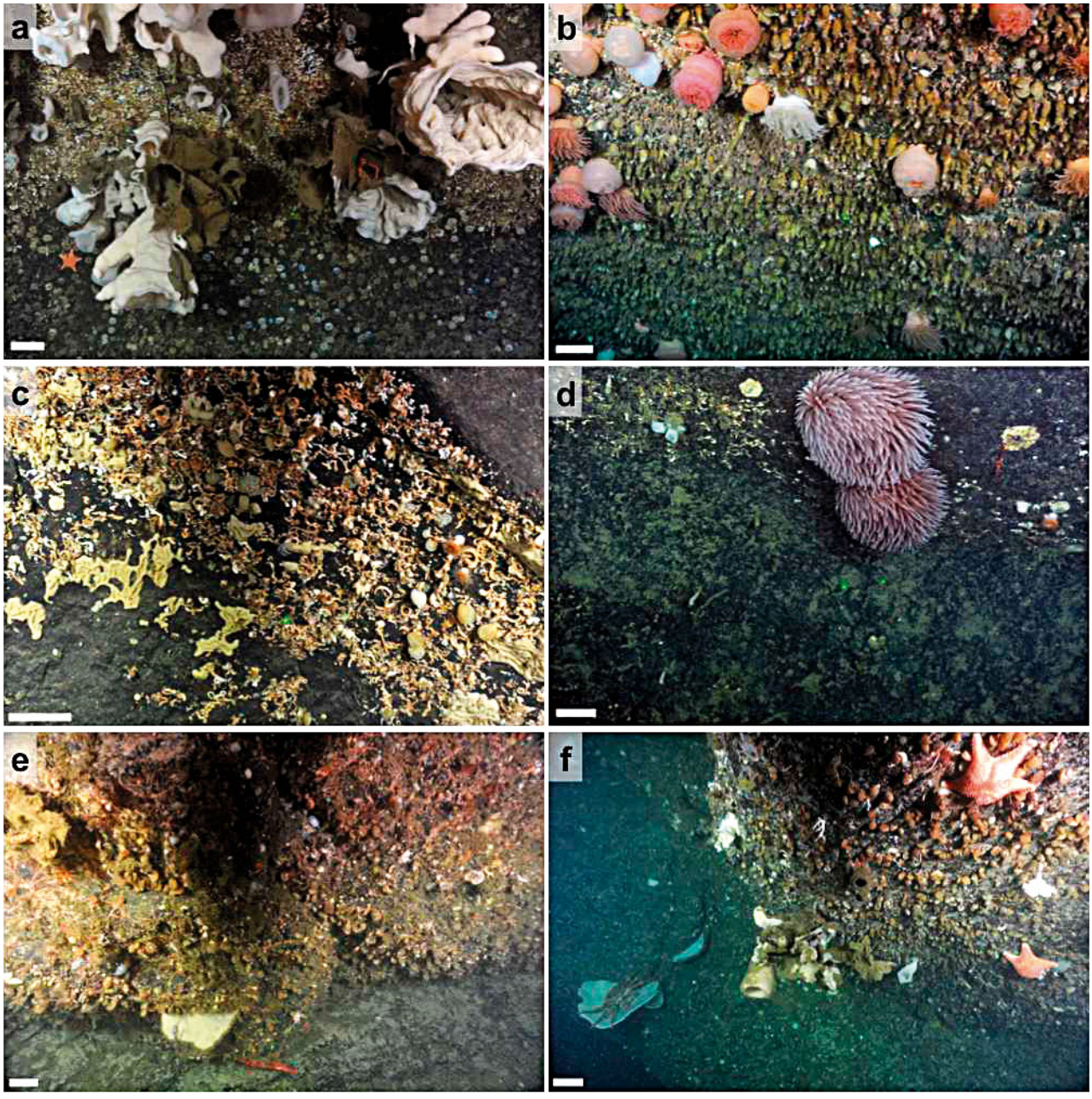

Fig. 4. Douglas Channel assemblages representative of depth zonation: (a,b) above 150 m, (c,d) 150 to 400 m, and (e,f) below 400 m. Scale bars: approx. 10 cm. Image contrasts are increased to account for backscatter in the water column. (a) Maitland Island: dense cover by hexactinellid sponges, serpulid tubes, and inarticulate brachiopods; (b) McKay Reach: zoanthid patches and anemones; (c) McKay Reach: articulate brachiopods, demosponges, and serpulid worms on slight overhang; (d) Maitland Island: lightly sedimented bedrock sparsely covered by demosponges and anemones; (e) Squally Reach: brittle stars, articulate brachiopods, cup corals, and a rockfish under a plate-like demosponge on a wall with accumulated sediment; (f) Squally Reach: asteroids, articulate brachiopods, brittle stars, a Dungeness crab, and an array of sponges on a deep wall

affinity include lyssacine glass sponges that occurred sporadically from ~200 m to the bottom of the Squally Reach transects, and the articulate brachiopod *Laqueus vancouveriensus* that had a near-ubiquitous presence below 200 m (Fig. 4c,e,f).

A few pairs of related taxa showed separation by depth. Above 200 m, the inarticulate brachiopod *Novocrania californica* was very common (Fig. 4a) at these depths, and articulate brachiopods decreased. The shift from articulate to inarticulate brachiopod

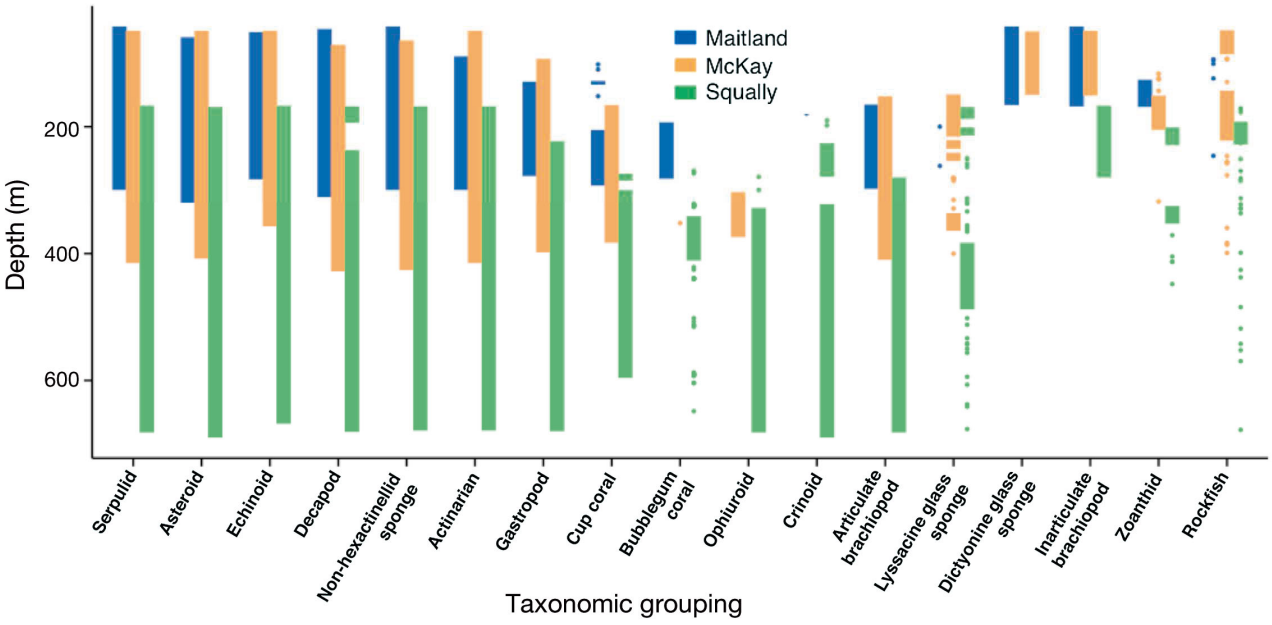

Fig. 5. General distributions of major taxonomic groups at each of the sites in Douglas Channel from continuous video presence/absence records. For a list of species that belong to each taxonomic group, see Table 1

presence occurred at ~150 to 180 m at Maitland and McKay and ~300 m at Squally. Rockfish below 200 m occurred in topographically complex areas (e.g. locations with step-relief, overhangs, or dead glass sponge skeletons), but were more common in shallower areas where biogenic habitats were more abundant. Dictyonine glass sponges dominated many of the steep-wall assemblages above 150 m, along with a unique co-occurring fauna that included relatively high densities of decapod crustaceans and rockfish (Fig. 5). Two numerous anthozoan taxa also had non-overlapping depth distributions; cup corals and zoanthids occurred mostly below and above ~200 m, respectively.

Mean animal cover estimates combined across all transects at the 3 sites were relatively low in the deeper reaches, then increased in variability both between and within depth bands around 250 m with a sharp mean increase at 150 m. Mean cover continued to increase incrementally above 100 m, and reached a maximum of 33% at 40 to 50 m (Fig. 6a). Depths below 400 m occurred only in the Squally Reach transects and small portions of the McKay Reach transects. In the 150 to 400 m depth ranges, no unique taxa were present, although arborescent corals were most commonly found here. While fewer taxonomic groups were present in the mid-depths (150 to 400 m) than the deep reaches, cover was similar and ranged from ~3 to 10% per 10 m depth band (Fig. 6a). Cosmopolitan groups such as articulate brachiopods, serpulid annelids, demosponges, actinarians, and gastropods dominated mid-depth walls. The sharp increase in cover seen at 150 m coincided with the appearance of dictyonine glass sponges, inarticulate brachiopods, and zoanthid patches, all of which reached high densities above 150 m. Encrusting sponges also became more abundant and larger, contributing to the high cover.

Percent animal cover was correlated with winter kinetic energy flux densities (linear regression, $F_{1,28} = 85.39$, $r^2 = 0.75$, $p < 0.001$), with a predicted percent cover of 7.56 + 18.14 × flux density (Fig. 6b) while summer fluxes were not ($p > 0.05$). The greatest landward (i.e. positive) fluxes occurred in the winter, while the strongest outflow fluxes were in summer (Fig. 6b).

Animal distributions in spaced still frames

Depth zonation was also evident in records of species abundances in 1 m^2 quadrats (Fig. 7). Sponge *Auletta krautteri* and pom-pom anemone *Cribrinopsis fernaldi* occurred throughout the depth range at low mean abundances when present (3.0 and 1.4 m^{-2}, respectively), with highest densities below 200 m. Arborescent corals were sparsely distributed; the small *Antipathes*, present only in Squally Reach quadrats, reached the highest densities at 189 m depth, and only *Primnoa pacifica* occurred in

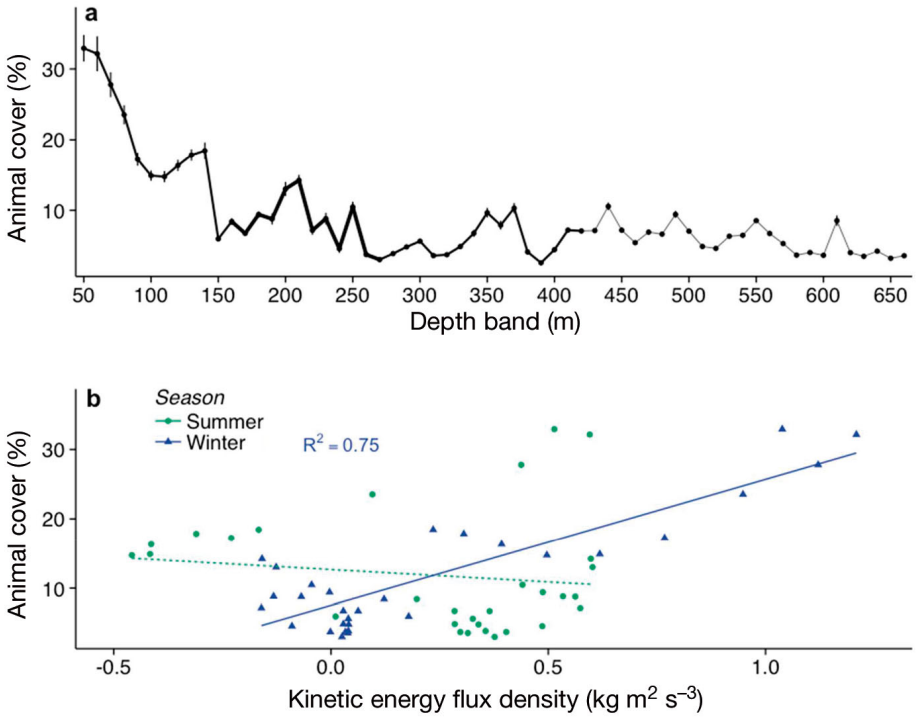

Fig. 6. (a) Mean animal % cover (±2 SE) by 10 m depth band composited across all sites estimated in every 10 s interval in the continuous video transects. Line weight increases with number of sites included in the depth band, with one being the thinnest line and 3 being the thickest. SE calculated from all transects available for a given depth band. Cover is relatively constant at all depths below 150 m, but increases shallower than 150 m. (b) Mean animal % cover versus mean seasonal kinetic energy flux density for each 10 m depth band. Kinetic energy flux values are from mooring KSK1; mean fluxes per 10 m depth band were calculated by averaging values in 1 m increments along spline interpolated line (see Fig. 3b) into 10 m bands. Solid and dashed lines show significant ($p < 0.05$) and non-significant ($p > 0.05$) linear regressions, respectively

quadrats above 150 m. A small number of species contributed to increasing densities in shallower water (Fig. 7). The brachiopod *L. vancouveriensus* was most abundant at 250 m, decreasing to low density patches (≤5 m^{-2}) above 150 m in cryptic environments (e.g. overhangs), while the inarticulate brachiopod *N. californica* densities below 200 m (≤30 m^{-2}) increased 3-fold above ~180 m at Maitland and McKay. Dense patches of the zoanthid *Epizoanthus scotinus* occurred primarily above 180 m further up the fjord. The encrusting sponges *Clathrina* cf. *coriacea* and *Plakina atka*, both nearly ubiquitous from 680 m upward, achieved their highest densities in the upper 150 m (Fig. 7); *P. atka* covered more than 25% of the available space in some areas. *Hexadella* spp., another encrusting sponge, showed similar space occupation with a peak around 200 m. Highest coverage by dictyonine glass sponges occurred in the shallowest portions of the transects as seen in the continuous assessment (Fig. 5).

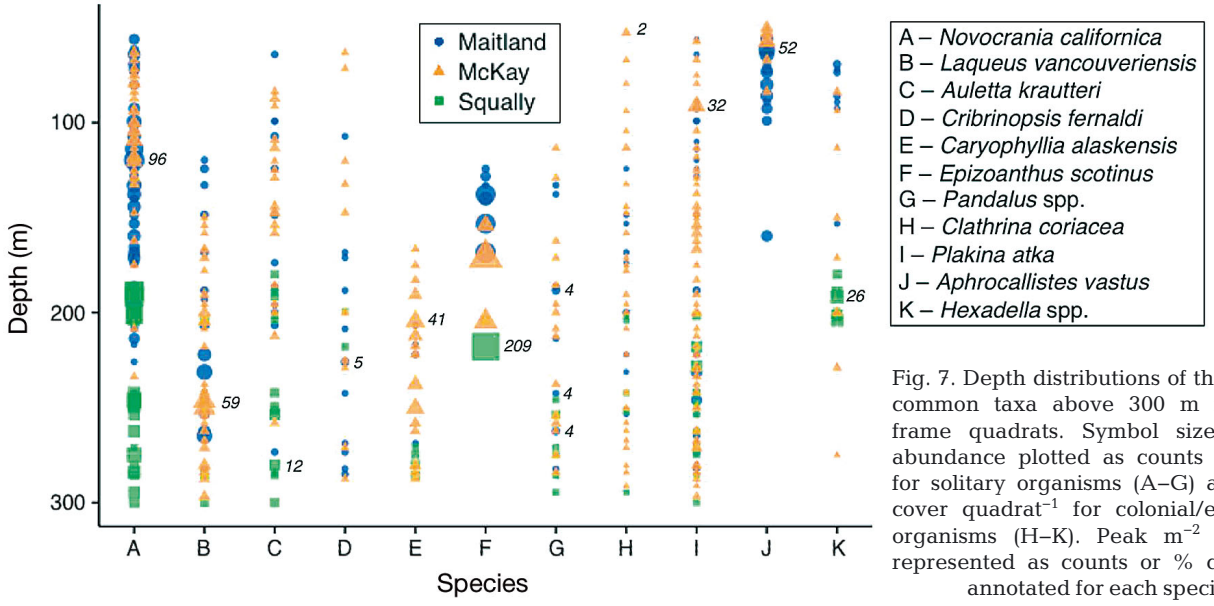

Fig. 7. Depth distributions of the 11 most common taxa above 300 m from still frame quadrats. Symbol size denotes abundance plotted as counts quadrat^{-1} for solitary organisms (A–G) and mean cover quadrat^{-1} for colonial/encrusting organisms (H–K). Peak m^{-2} densities, represented as counts or % cover, are annotated for each species

Distinct species assemblages

PERMDISP analysis of quadrats showed no significant dispersions for the 'site' factor ($F_{2,232}$ = 0.42553, p[perm] = 0.647). Although the subsequent PERMANOVA results indicate that animal assemblages were significantly structured by site (Pseudo-F = 11.467, df = 2, SS = 68 289, MS = 34 144, p[perm] = 0.001), CAP-visualization of our cluster analysis displayed substantial overlap among the assemblages at the 3 sites with little apparent pattern of clustering in the site-level structure of quadrat assemblages (Fig. 8a). However, clustering was more apparent from 175 to 300 m, where the 3 sites overlap (Fig. 8b).

Cluster analysis and the subsequent SIMPER test identified the taxa that contributed most to the similarity between 25 m depth bands at each site (Table 3). The demosponge *P. atka* contributed most to the among-depth-band similarity at McKay and Squally, while the inarticulate brachiopod *N. californica* was the largest contributor for Maitland quadrats.

SIMPROF analysis displayed 6 unique assemblages in quadrats across the 3 sites (Fig. 8c), and the consequent SIMPER analysis described the taxa comprising each group (Table 4). Similarity within assemblage VI, the most common in the fjord, was driven by the near-ubiquitous *P. atka* and species that occurred from mid-depths down. Assemblage V, the second most common, was dominated by *N. californica*, the inarticulate brachiopod that primarily occurred above ~150 m. No assemblages were unique to one site, although assemblage I, composed primarily of mobile species, was not present at Maitland Island. The uncommon I and III assemblages were associated with sparse cover and composed of few species. More than 80% of the similarity among quadrats within the II, IV, and V assemblages was driven by a single species (*Hexadella* spp., *E. scotinus*, and *N. californica*, respectively).

The best DistLM model included all but one of the null model environmental parameters (R^2 = 0.22, RSS = 5.94 × 10^5; in order of decreasing explanations of variance: depth, animal cover, temperature, relief and dissolved oxygen; Table 5). A dbRDA plot (Fig. 8d) shows the contributions of each variable to the model, in which assemblage VI associated most closely with the depth vector. All other assemblages

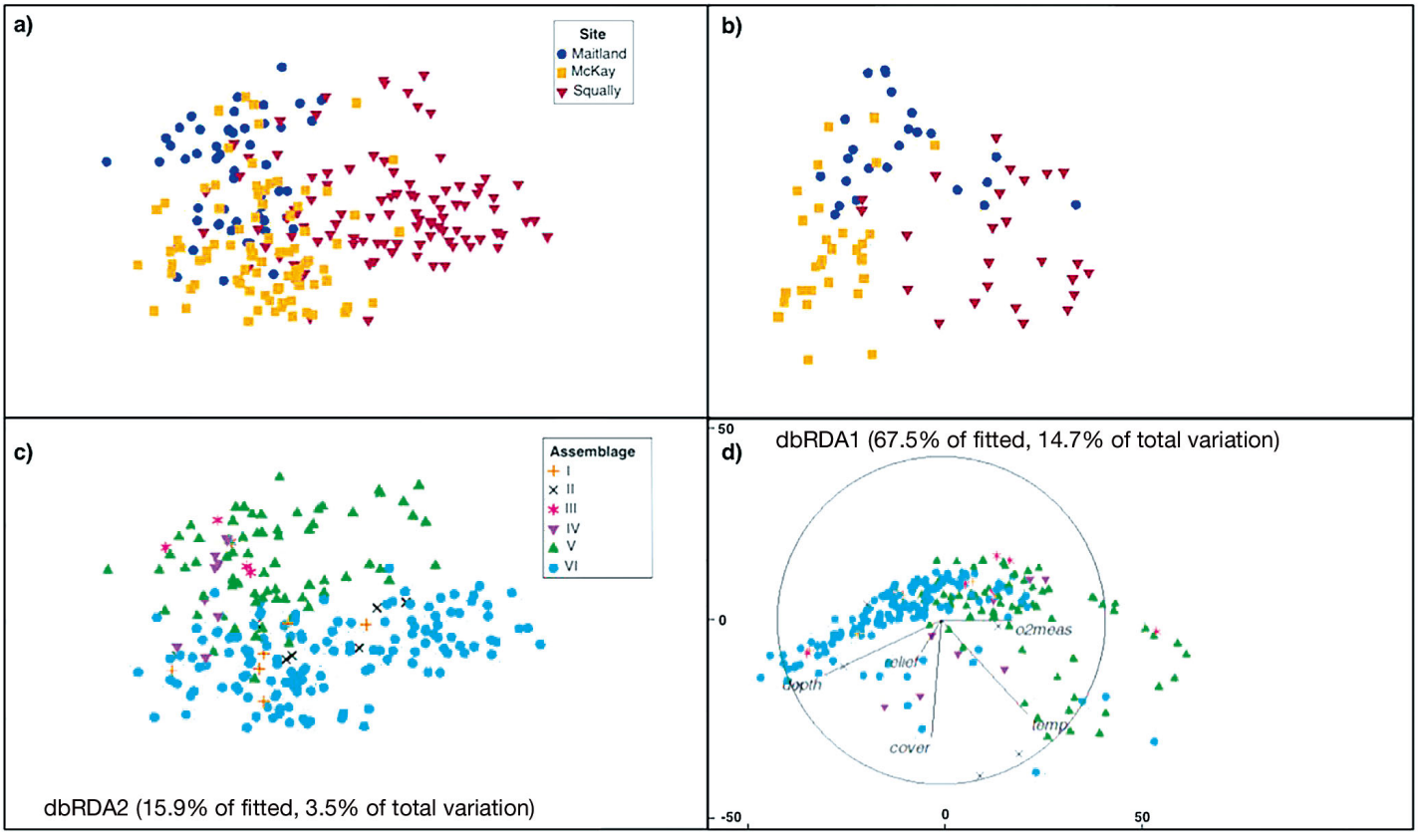

Fig. 8. Canonical analysis of principal coordinates (CAP) plots based on Bray-Curtis similarity of quadrat samples examined by (a) site (all depth ranges), and (b) site (overlapping depth ranges, i.e. 175–300 m) (c) SIMPROF-determined assemblages (I–VI; see Table 4). (d) Distance-based redundancy analysis (dbRDA) plot of DistLM results in 2 dimensions using assemblages I to VI. Length of variable vector is proportional to contribution to the total explained variance (see Table 5)

Table 3. Taxon composition by SIMPER for 25 m depth band comparisons among and between sites. Group similarity is among 25 m depth bands at each site; pairwise similarity is between 25 m depth bands between sites. Cut-off for cumulative percentage to group similarity: 95%. Species contributing over 10% are brachiopods (*Novocrania californica* and *Laqueus vancouveriensus*), sponges (*Plakina atka* and *Clathrina* cf. *coriacea*) and the cup coral, *Caryophyllia alaskensis*

Assemblage	Average pairwise similarity (%)	Group similarity (%)	Taxa (contributing % similarity)
Maitland	McKay – 18.1 Squally – 17.3	25.4	*N. californica* (61.9), *P. atka* (14.9), *L. vancouveriensus* (6.4), dictyonines (3.4), *Auletta krautteri* (3.1), *Cribrinopsis fernaldi* (2.0), *Epizoanthus scotinus* (1.4), *Strongylocentrotus pallidus* (1.0), *Clathrina coriacea* (1.0)
McKay	Squally – 21.5	23.9	*P. atka* (44.5), *L. vancouveriensus* (16.2), *C. coriacea* (13.9), *N. californica* (7.0), *C. alaskensis* (6.5), *A. krautteri* (3.1), *Pandalus* (3.0), *S. pallidus* (1.1)
Squally	–	26.2	*P. atka* (24.9), *C. alaskensis* (13.9), *C. coriacea* (10.4), *N. californica* (10.1), *L. vancouveriensus* (6.6), *Ophiopholis aculeata* (6.4), *Hexadella* (4.9), *A. krautteri* (4.7), *Calliostoma platinum* (4.1), *Antipathes* (3.8), Porifera1 (3.6), *Pandalus* (2.4)

Table 4. Taxon composition by SIMPER for the similarity profile (SIMPROF)-determined assemblages (I–VI). Group similarity is between quadrats within the assemblage group; cut-off for cumulative percentage to group similarity: 95%

Assemblage	Group similarity (%)	Taxa (contributing % similarity)
I	32.0	*Pandalus* (71.2), *Fusitron oregonensis* (11.5), *Caryophyllia alaskensis* (6.5), *Ophiopholis aculeata* (5.8)
II	33.5	*Hexadella* (86.2), dictyonines (3.3), *C. alaskensis* (2.1), *Cribrinopsis fernaldi* (1.4)
III	50.0	*C. fernaldi* (78.1), *Novocrania californica* (21.9)
IV	48.5	*Epizoanthus scotinus* (80.8), *N. californica* (11.1), *Laqueus vancouveriensus* (2.5), *Plakina atka* (1.8)
V	40.9	*N. californica* (80.7), *P. atka* (7.0), *Auletta krautteri* (4.6), *Clathrina coriacea* (1.4), *Strongylocentrotus pallidus* (1.1), dictyonines (1.0)
VI	30.6	*P. atka* (42.5), *L. vancouveriensus* (16.4), *C. coriacea* (12.8), *C. alaskensis* (11.8), *O. aculeata* (3.3), *Calliostoma platinum* (2.5), *A. krautteri* (2.5), *Pandalus* spp. (1.7), Porifera1 (1.30), *Hexadella* (1.1)

displayed no apparent trend along the environmental variable vectors.

Functional and taxonomic diversity

Significant differences between sites in the 25 m depth bands were shown for mean sUTC (Welch's ANOVA, $F = 7.96$, df = 2, 22.51, $p < 0.01$) and species richness (Welch's ANOVA, $F = 6.84$, df = 2, 23.70, $p < 0.01$); Squally Reach had a significantly greater mean value than the other sites for both sUTC and species richness (Games-Howell post hoc test, $p < 0.05$ for both; Fig. 9a,d). Taxonomic distinctness (Δ+), on the other hand, was not significantly different between sites (Welch's ANOVA; $p > 0.05$), and had high (>90%) median values at each site (Fig. 9b). Neither FDis (Fig. 9c) nor FEve differed significantly between

Table 5. Distance-based linear model pseudo-*F* values and the amount of variance explained by each variable selected by DistLM as part of the best model

Environmental variable	Pseudo-*F*	Proportion of explained variance	Cumulative explained variance
Depth	32.53	0.12	0.12
% Animal cover	9.43	0.034	0.16
Temperature	9.42	0.033	0.19
Relief	4.36	0.015	0.20
Dissolved oxygen	3.78	0.013	0.22

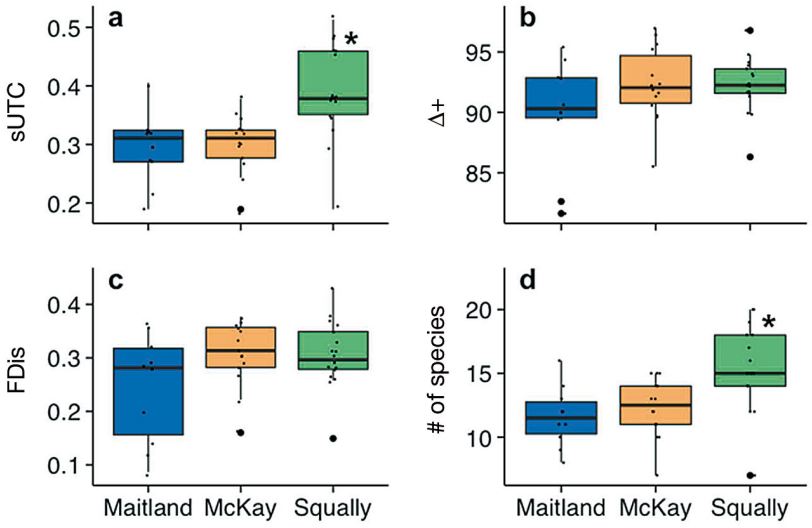

Fig. 9. Site-by-site comparisons of taxa scored in quadrats. Variables were calculated for 25 m depth bands. Bolded black lines: median values; upper and lower edges of the boxes: 2nd and 3rd quartiles of the data, respectively; whiskers: edges of the 1st and 4th quartiles; large dots: outliers; small dots: data points. Asterisks: significant differences between sites as determined by Welch's ANOVA ($p < 0.05$). (a) Unique trait combinations in a sample versus the entire species pool (sUTC); (b) taxonomic distinctness (Δ+); (c) functional dispersion (FDis); and (d) number of species

sites (Welch's ANOVA, $p > 0.05$), although FDis was more varied at Maitland.

There were no obvious trends with depth for FEve, FDis, and Δ+, but sUTC and sΔ+ decreased sharply above ~325 m at Squally Reach (Fig. 10a). Both sUTC and sΔ+ were similar between Maitland and McKay at all depth bands deeper than 100 to 125 m, and both steadily decreased at McKay above 175 m with an increase in the uppermost 50 to 75 m depth band. Quadrats shallower than 200 m had significantly lower values for both sUTC and sΔ+ (ANOVA; $F_{1,39}$ = 8.38 and 7.51, respectively; $p < 0.01$ for each; Fig. S1). There were no apparent trends with depth for FEve or FDis, but 3 of the 4 depth bands with Δ+ below the calculated expected value of Δ+ (i.e. under the assumption of random assembly from the entire species pool) were above 100 m (Fig. S2). sUTC and the number of species per 25 m depth band were significantly positively correlated, suggesting unused trait combinations and a low level of functional redundancy at the depth band scale (Spearman's rank correlation = 0.96, $p < 0.01$; Fig. 10b).

DISCUSSION

This first record of the deep hard substratum fauna in the Douglas Channel complex reveals a suite of diverse assemblages marked by vertical zonation, expanses with dense cover, and variation along the fjord head-mouth axis. We recorded 53 species (or species groups) representing 9 phyla and 38 orders from the 9 transects. The spatial dominance by large sessile invertebrates and the lack of evidence for recent mass recruitments

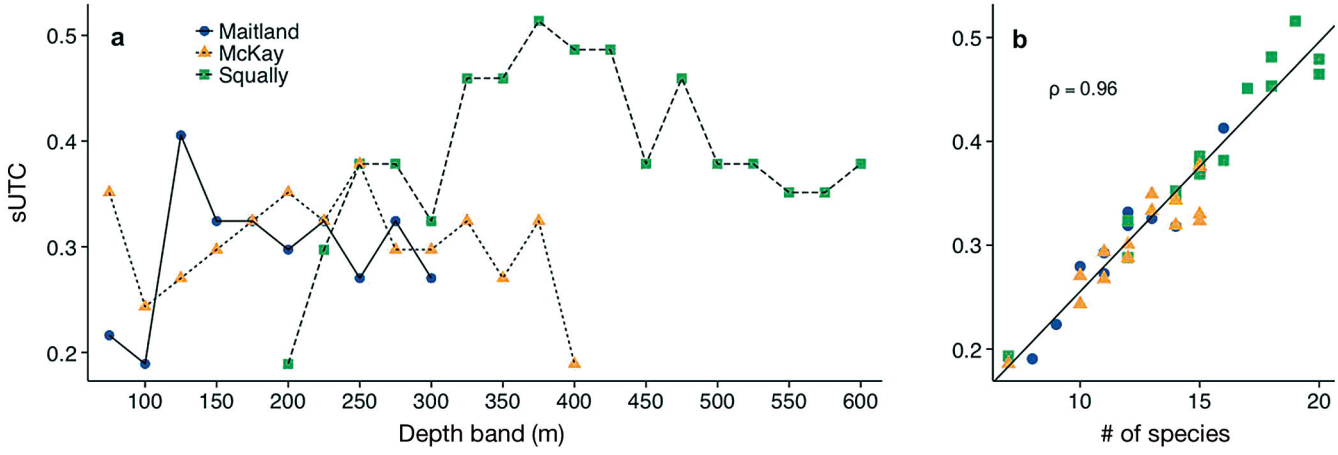

Fig. 10. (a) Proportions of unique trait combinations (sUTC) by depth band and location. Depth labels represent the base of each band. Both sUTC and taxonomic distinctness × richness (sΔ+; not shown) identify greater diversity below 300 m in Squally Reach than at all other depths in the fjord. (b) Relationship between sUTC and number of species in each 25 m depth band. The linear relationship proceeds throughout the entire range of species richness, indicating low functional redundancy at the depth band scale at all sites

indicate that these assemblages are primarily composed of perennial species, and thus are shaped over long timescales.

Vertical walls form a substantial component of the total benthic habitat in fjordic environments. We estimated, using the mean depth and coastline length of Douglas Channel from Macdonald et al. (1983), that walls represent ~20% of the fjord's total benthic area; the majority of these cliffs surveyed in the current study were unsedimented (Table S1), and thus available for colonization. Although this estimate may be high due to our site selection for steep topography, most low-relief walls with moderate-to-heavy sediment drape were colonized by organisms while adjacent flat areas were not. Guided submersible systems are required to investigate these steep bedrock substrata, as standard deep-sea sampling techniques (e.g. grabs, towed camera systems, etc.) do not suffice. For this reason, the contribution of deep wall habitats to ecosystem diversity and function remains nearly unknown.

Depth-related distributions

Most of the mobile species and larger sessile animals documented were eurybathic, but some taxa (6 of the 17 documented groups) were primarily seen below 400 m. As only Squally Reach extended below 400 m, it is possible that these taxa were also constrained by site (near the fjord mouth) as well as depth. The bubblegum coral *Paragorgia arborea* and crinoid *Florometra serratissima*, for example, were primarily seen from 200 m to below 600 m and at Squally Reach, but records of these species exist in shallower waters (e.g. Stone 2014), including elsewhere in Douglas Channel (R. Gasbarro unpubl. data).

Mean animal cover above 150 m reached a peak at 40 to 50 m nearly 3 times that of the average cover across all depths. High densities of glass sponges in the upper 150 m are similar to those in Leys et al. (2004), who surveyed 11 BC fjords and found the highest densities of glass sponges from 50 to 150 m in Jervis Inlet. Amongst solitary epilithos, only the inarticulate brachiopod *Novocrania californica* noticeably increased in the upper 150 m. Tunnicliffe & Wilson (1988) also found a shallow water distinction and high densities of *N. californica* in nearby Dean and Burke Channels. As the lower valve of craniid brachiopods cements to the wall, feeding takes place very low in the boundary layer compared to terebratulids; thus, access to suspended particles in turbulent flow may affect this distribution.

The increase in animal cover with kinetic energy flux density above 150 m indicates that these animals benefit from increased particle delivery due to consistent estuarine inflow. While kinetic energy flux is confounded with depth in the upper ~200 m, the relationship between depth and animal cover is much weaker than that of kinetic energy flux and animal cover, suggesting that there is a measurable effect of kinetic energy flux on the high animal densities at these depths. Enhanced turbulence at these intermediate depths will also increase substratum contact frequency by settling larvae (Abelson & Denny 1997) without impeding suspension-feeding functions, as inflow velocities rarely exceed 20 cm s^{-1} (Wan et al. 2017). The positive correlation with winter flux density suggests that incoming storm-mixed oceanic water may be more important for suspension-feeder growth than outflowing water that contains greater concentrations of low-nutrient riverine particulates (Johannessen et al. 2015). However, in the summer, higher density diel vertical zooplankton migrations are another important component of the seston pool available to suspension feeders, and their daytime descents are also limited to the upper ~150 m of the fjord (Keen et al. 2017). Thus, the physical dynamics of the fjord appear to exert a strong influence on the wall assemblages, likely with enhanced food delivery shallower than 150 m supporting higher biomass.

Sharp increases in kinetic energy flux density, overall animal cover, and food-limited species all suggest a switch from the food-limited assemblages below ~150 m to assemblages that primarily compete for space where cover reached >80% in some areas. These densities rival those of productive ecosystems such as coral reefs, where competition for space is fierce (Chadwick & Morrow 2011). Quadrats with ≥50% animal cover never contained fewer than 3 species, even when a single organism primarily occupied the space. Indeterminate lateral growth and clonal strategies (Sebens 1987) were common amongst the high space occupiers (e.g. encrusting sponges, zoanthids). Solitary species that form dense monospecific aggregations also prevent overgrowth from other species (Jackson 1977), such as serpulid worms and inarticulate brachiopods in Douglas Channel. Glass sponges and some demosponges escape from competition by growing off the substratum (Sebens 1982). Monitoring efforts of these deep wall fauna would be useful in assessing the role and mechanisms of space competition most important in structuring the assemblages.

Site differences

While the PERMANOVA revealed a significant site effect, effect size was somewhat small, indicating relatively mild differences between sites along the fjord axis. The most obvious difference between sites was due to the great densities of inarticulate brachiopods at Maitland that drove the multivariate community structure here, while the encrusting demosponge *Plakina atka* was dominant at the other sites (Table 3). Brachiopods maintain high densities at the heads of other BC fjords where high sedimentation rates exclude less tolerant epifauna (Tunnicliffe & Wilson 1988, Farrow et al. 1983). Although terrigenous input into Douglas Channel is lower relative to glacially fed BC inlets (Macdonald et al. 1983), some epifauna are likely intolerant of settling sediment disturbance at the fjord head, to the benefit of *N. californica*. The spring freshet causes sinking particle pulses of up to 5 g m^{-2} d^{-1} (Johannessen et al. 2015). While less than the average inputs into fjords that drain ice fields (Farrow et al. 1983), these pulses may represent significant periodic disturbances that shape the animal assemblages near the fjord head.

The increase in species richness at the seaward end of the fjord may be driven by greater concentrations of chlorophyll *a* and zooplankton in the outer fjord basin (Keen et al. 2017). Proximity to the outer sill may enhance larval delivery to Squally Reach from Hecate Strait, as found by Quijon & Snelgrove (2005) in a Newfoundland fjord system. Alternatively, the greater richness at Squally may be due to the addition of echinoderms and corals with affinities to the greater depth at this site. Explicit tests of these relationships in future studies would enhance our understandings of the diversity patterns in Douglas Channel.

Functional diversity

As body form diversity is an important feature of suspension-feeder assemblages, it can serve as a proxy for trophic structure (Gili & Coma 1998). The low functional redundancy within quadrats (Fig. 10b) indicates that even where many species occupied the walls, body forms were varied. The lack of functional redundancy was also evident in the taxonomic distinctness × richness (sΔ+) index that mirrored the sUTC index; where species increased, so did functional richness and sΔ+. The high taxonomic distinctness at the depth-band scale throughout the fjord (Fig. S2) also highlights the diversity of lineages that have adopted the suspension-feeding mode, along with a variety of mobile predators. This morphological diversity may allow for resource partitioning by consumption of varied particle sizes (Abelson et al. 1993), with the multiple modes of suspension feeding by zoobenthos (Riisgård & Larsen 2000) leading to wide differences in foraging efficiency, energetics, and consumed seston fractions (Coma et al. 2001). The relatively low mean FDis (~0.3) suggests that, per depth band, the abundance-weighted divergences in species traits within assemblages were relatively small, and that changes in traits expressed by assemblages primarily occurred over depth ranges larger than 25 m.

The distinct deep 'VI' assemblage at Squally Reach encompassed traits that reflect habitat formation including various arborescent and cup corals with high abundances of ophiuroids, and both free-living and epizootic crinoids. These organisms had unique trait combinations that were absent or rare on mid-depth walls where encrusting organisms dominated, and drove the high sUTC below 300 m in Squally Reach. They also all either create 3-dimensionality off the walls, or, in the case of the ophiuroids, favor areas where significant 3-dimensionality is present. While not numerically dominant, glass sponges (Marliave et al. 2009) and arborescent corals (Stone 2014) are important habitat formers where relatively high densities of rockfish and decapod crustaceans occur.

Ecological relevance of fjord walls

Fjords provide sheltered waters with expanses of near vertical, unsedimented bedrock across large depth ranges that can be readily colonized. These cliffs can foster high-biomass assemblages that are distinct from the sedimented fjord floor. Habitat complexity is increased by the erect morphologies of many of the sessile organisms, and the microhabitats they provide are used by commensals as refuges; in some cases, these interactions are even mutualistic (Buhl-Mortensen et al. 2010). Crinoids and zoanthids were seen attached to various erect sponges, while brittle stars, echinoids, decapods, and rockfish achieved their greatest densities where 3-dimensional biological structures were present.

Fjords provide habitat for a variety of organisms known mostly in offshore deep-water settings. The Brachiopoda, once dominant in Paleozoic subtidal assemblages, are rare components of Holocene ecosystems, yet they are nearly ubiquitous in British Columbian fjords such as Douglas Channel (Tunni-

cliffe & Wilson 1988), and maintain dense populations in the fjords of Chile (Baumgarten et al. 2014) and New Zealand (Richardson 1981). Glass sponges are mostly deep-sea taxa, but occur at shallow depths throughout the BC coast/shelf and form extensive reefs in some areas (Leys et al. 2004). Southward & Southward (1992) reported a pogonophoran tubeworm from 200 to 300 m in 2 northern BC fjords that was previously known from deep-sea environments. Fjord biota are also reservoirs of genetic diversity (Turan et al. 1998, Drengstig et al. 2000, Le Goff-Vitry et al. 2004); allopatric speciation (Suneetha & Naevdal 2001) and pre-acclimation to ocean acidification (Fillinger & Richter 2013) may occur in isolated fjordic populations.

Bentho-pelagic coupling, while not directly measured in this study, likely exerts a strong influence over the carbon flow and productivity of the fjord. The high suspension-feeder abundance, especially in the upper 150 m, transforms sinking organic matter and plankton into benthic biomass, some of which becomes available to larger predators. Subsequent release to the pelagic system of waste products, gametes, and larvae maintains organic cycling within the fjord before final loss to bottom sediments (Perea-Blázquez et al. 2012) or flushing. Our results suggest that the breadth of biofiltration may be greatest in the deepest portion of the fjord where there is the greatest array of body forms, but that nutrient fluxes likely increase above ~150 m where abundances, especially sponges, were greatest. Sponges have some of the highest capture rates measured for any suspension-feeding taxa, and thus are significant regulators of seston in the water column (Gili & Coma 1998, Yahel et al. 2007, Kahn et al. 2015). More specific measurements of community filtration rates would be useful for further functional characterization of the wall fauna.

Numerous development projects, including the proposed diluted bitumen (dilbit) pipeline terminus and liquefied natural gas (LNG) plants at the fjord head, would bring heavy tanker traffic into Douglas Channel (Enbridge 2010). Better understanding of the consequences of petroleum product spills in aquatic environments requires baseline benthic studies (Lee et al. 2015). A 2010 Kalamazoo River spill of dilbit had toxicological effects on organisms from microbes to chordates, and cleanup required years of dredging, arguably causing ecological impacts as great as the original spill (Dew et al. 2015). A dilbit spill in Douglas Channel may possibly sink (Wu et al. 2016). In 2016, a ban on oil tankers came into effect (House of Commons Canada 2017). Thus, such risks will remain low as long as the ban is maintained.

These first surveys of the deep wall fauna of Douglas Channel augment our understanding of the distribution of northeast Pacific coastal diversity. Differences are emerging in faunal composition and environmental forcing along the coast. Douglas Channel is relatively oligotrophic (Wright et al. 2016), and nutrient regeneration largely comes from adjacent shelf water, concentrating nutrients at depth (Johannessen et al. 2015). Oxygen in the fjord was comparable to Jervis Inlet, where low productivity and a deep basin prevent large fluxes of organic matter from depleting bottom oxygen (Timothy et al. 2003). Conversely, high productivity southern fjords such as Saanich Inlet and the inner basin of Howe Sound support dense vertical-wall communities even under periodic oxygen depletion (Tunnicliffe 1981, Levings et al. 1983). Douglas Channel and other northern BC fjords host inarticulate brachiopods, zoanthids, pom-pom anemones, crinoids, and brittle stars in great abundances, whereas they are rare or absent in southern BC and Vancouver Island fjords (Levings et al. 1983). Southern fjords also have high densities of an articulate brachiopod *Terebratulina unguicula* (Tunnicliffe & Wilson 1988) and ascideans (Tunnicliffe 1981); the former was absent and the latter rare in Douglas Channel. While the taxa in Douglas Channel matched those seen in nearby inlets and none appeared to be exclusive to the fjord, the overall species diversity was lower than that seen in other northern (V. Tunnicliffe unpubl. data.) and southern (Levings et al. 1983) BC fjords.

The distinct assemblage profiles and environmental uniqueness of fjords, along with the high animal densities highlight the importance of this fjordic wall fauna to the coastal diversity of the northeast Pacific. Furthermore, several taxa listed as 'vulnerable' (e.g. glass sponges and tree corals; Fisheries and Oceans Canada 2010) are present on the Douglas Channel cliffs. Fjord walls are high biomass, high functioning, and expansive systems that may act as biodiversity reservoirs in a changing ocean, warranting consideration when developing management profiles for coastal oceans.

Acknowledgements. We are grateful for the field support from the Canadian Scientific Submersible Facility and the captains and crew of the CCGS 'Tully'. Thanks to J. Rose, C. Du Preez, and J. Pegg for dive-logging and technical support. R.G. thanks R. Boschen for a primer on PRIMER. H. Reiswig and B. Stone provided help with sponge identifications. Many thanks to S. K. Juniper, J. Baum, A. Sastri and C. Hannah, whose notes helped improve draft versions of the manuscript. This work was supported by Fisheries and Oceans Canada and the Natural Research and Engineering Research Council Canada.

LITERATURE CITED

Abelson A, Denny M (1997) Settlement of marine organisms in flow. Annu Rev Ecol Syst 28:317–339

Abelson A, Miloh T, Loya Y (1993) Flow patterns induced by substrata and body morphologies of benthic organisms, and their roles in determining availability of food particles. Limnol Oceanogr 38:1116–1124

Anderson MJ (2006) Distance-based tests for homogeneity of multivariate dispersions. Biometrics 62:245–253

Anderson JJ, Devol AH (1973) Deep water renewal in Saanich Inlet, an intermittently anoxic basin. Estuar Coast Mar Sci 1:1–10

Anderson M, Gorley R, Clarke KP (2008) PERMANOVA+ for PRIMER: guide to software and statistical methods. PRIMER-E, Plymouth

Baumgarten S, Laudien J, Jantzen C, Haeussermann V, Foersterra G (2014) Population structure, growth and production of a recent brachiopod from the Chilean fjord region. Mar Ecol 35:401–413

Boje J, Neuenfeldt S, Sparrevohn CR, Eigaard O, Behrens JW (2014) Seasonal migration, vertical activity, and winter temperature experience of Greenland halibut *Reinhardtius hippoglossoides* in West Greenland waters. Mar Ecol Prog Ser 508:211–222

Buhl-Mortensen L, Vanreusel A, Gooday AJ, Levin LA and others (2010) Biological structures as a source of habitat heterogeneity and biodiversity on the deep ocean margins. Mar Ecol 31:21–50

Buss LW (1990) Competition within and between encrusting clonal invertebrates. Trends Ecol Evol 5:352–356

Carney D, Oliver JS, Armstrong C (1999) Sedimentation and composition of wall communities in Alaskan fjords. Polar Biol 22:38–49

Chadwick NE, Morrow KM (2011) Competition among sessile organisms on coral reefs. In: Dubinsky Z, Stambler N (eds) Coral reefs: an ecosystem in transition. Springer, Dordrecht, p 347–371

Clague JJ (1985) Deglaciation of the Prince Rupert–Kitimat area, British Columbia. Can J Earth Sci 22:256–265

Clarke KR, Gorley RN (2006) PRIMER v6: user manual/tutorial. Plymouth Marine Laboratory, Plymouth

Clarke KR, Warwick RM (2001) A further biodiversity index applicable to species lists: variation in taxonomic distinctness. Mar Ecol Prog Ser 216:265–278

Coma R, Ribes M, Gili JM, Hughes RN (2001) The ultimate opportunists: consumers of seston. Mar Ecol Prog Ser 219:305–308

Dew WA, Hontela A, Rood SB, Pyle GG (2015) Biological effects and toxicity of diluted bitumen and its constituents in freshwater systems. J Appl Toxicol 35:1219–1227

Drengstig A, Fevolden SE, Galand PE, Aschan MM (2000) Population structure of the deep-sea shrimp (*Pandalus borealis*) in the north-east Atlantic based on allozyme variation. Aquat Living Resour 13:121–128

Enbridge (2010) Volume 8A: overview and general information — marine transportation. Enbridge Northern Gateway Project Sec. 52 Application. Enbridge Northern Gateway Pipelines, Calgary

Farrow G, Syvitski J, Tunnicliffe V (1983) Suspended particulate loading on the macrobenthos in a highly turbid fjord: Knight Inlet, British Columbia. Can J Fish Aquat Sci 40(Suppl 1):273–288

Fillinger L, Richter C (2013) Vertical and horizontal distribution of *Desmophyllum dianthus* in Comau Fjord, Chile: a cold-water coral thriving at low pH. PeerJ 1:e194

Fisheries and Oceans Canada (2010) Pacific region cold-water coral and sponge conservation strategy: 2010–2015. Fisheries and Oceans Canada, Vancouver

Genin A, Paull C, Dillon W (1992) Anomalous abundances of deep-sea fauna on a rocky bottom exposed to strong currents. Deep-Sea Res A Oceanogr Res Pap 39:293–302

Gili JM, Coma R (1998) Benthic suspension feeders: their paramount role in littoral marine food webs. Trends Ecol Evol 13:316–321

Haedrich R, Gagnon J (1991) Rock wall fauna in a deep Newfoundland fjord. Cont Shelf Res 11:1199–1207

Hart DD, Finelli CM (1999) Physical-biological coupling in streams: the pervasive effects of flow on benthic organisms. Annu Rev Ecol Syst 30:363–395

Hooper DU, Chapin FS, Ewel JJ, Hector A and others (2005) Effects of biodiversity on ecosystem functioning: a consensus of current knowledge. Ecol Monogr 75:3–35

House of Commons Canada (2017) Bill C-48: Oil Tanker Moratorium Act. 1st Reading May 12, 2017, 42nd Parliament, 1st session. www.parl.ca/DocumentViewer/en/42-1/bill/C-48/first-reading

Hughes JD (2015) A clear look at BC LNG: energy security, environmental implications and economic potential. Canadian Centre for Policy Alternatives, BC Office. www.northwestinstitute.ca/index.php/lng

Huvenne VAI, Tyler PA, Masson DG, Fisher EH and others (2011) A picture on the wall: innovative mapping reveals cold-water coral refuge in submarine canyon. PLOS ONE 6:e28755

Jackson JBC (1977) Competition on marine hard substrata: the adaptive significance of solitary and colonial strategies. Am Nat 111:743–767

Jantzen C, Haeussermann V, Foersterra G, Laudien J, Ardelan M, Maier S, Richter C (2013) Occurrence of a cold-water coral along natural pH gradients (Patagonia, Chile). Mar Biol 160:2597–2607

Johannessen SC, Wright CA, Spear DJ (2015) Seasonality and physical control of water properties and sinking and suspended particles in Douglas Channel, British Columbia. Canadian Technical Report of Hydrography and Ocean Sciences No. 308. Fisheries and Oceans Canada, Sidney

Kahn AS, Yahel G, Chu JWF, Tunnicliffe V, Leys SP (2015) Benthic grazing and carbon sequestration by deep-water glass sponge reefs. Limnol Oceanogr 60:78–88

Keen EM, Wray J, Meuter H, Thompson KL, Barlow JP, Picard CR (2017) 'Whale wave': shifting strategies structure the complex use of critical fjord habitat by humpbacks. Mar Ecol Prog Ser 567:211–233

Keyel AC, Wiegand K (2016) Validating the use of unique trait combinations for measuring multivariate functional richness. Methods Ecol Evol 7:929–936

Kundu PK, Cohen IM (2008) Fluid mechanics, 4th edn. Academic Press, Amsterdam

Laliberté E, Legendre P (2010) A distance-based framework for measuring functional diversity from multiple traits. Ecology 91:299–305

Le Goff-Vitry MC, Pybus OG, Rogers AD (2004) Genetic structure of the deep-sea coral *Lophelia pertusa* in the northeast Atlantic revealed by microsatellites and internal transcribed spacer sequences. Mol Ecol 13:537–549

Lee K, Boufadel M, Chen B, Foght J, Hodson P, Swanson S, Venosa A (2015) The behaviour and environmental impacts of crude oil released into aqueous environments.

Expert panel report, Royal Society of Canada, Ottawa
Leichter JJ, Witman JD (1997) Water flow over subtidal rock walls: relation to distributions and growth rates of sessile suspension feeders in the Gulf of Maine. Water flow and growth rates. J Exp Mar Biol Ecol 209:293–307
Lesser MP, Witman JD, Sebens KP (1994) Effects of flow and seston availability on scope for growth of benthic suspension-feeding invertebrates from the Gulf of Maine. Biol Bull (Woods Hole) 187:319–335
Levings C, Foreman R, Tunnicliffe V (1983) Review of the benthos of the Strait of Georgia and contiguous fjords. Can J Fish Aquat Sci 40:1120–1141
Leys SP, Wilson K, Holeton C, Reiswig HM, Austin WC, Tunnicliffe V (2004) Patterns of glass sponge (Porifera, Hexactinellida) distribution in coastal waters of British Columbia, Canada. Mar Ecol Prog Ser 283:133–149
Macdonald RW, Bornhold BD, Webster I (1983) The Kitimat fjord system: an introduction. In: Proceedings of a Workshop on the Kitimat Marine Environment. Can Tech Rep Hydrogr Ocean Sci 18:3–13
Marliave JB, Conway KW, Gibbs DM, Lamb A, Gibbs C (2009) Biodiversity and rockfish recruitment in sponge gardens and bioherms of southern British Columbia, Canada. Mar Biol 156:2247–2254
Miller RJ, Etter RJ (2011) Rock walls: small-scale diversity hotspots in the subtidal Gulf of Maine. Mar Ecol Prog Ser 425:153–165
Moon HW, Hussin WMRW, Kim HC, Ahn IY (2015) The impacts of climate change on Antarctic nearshore megaepifaunal benthic assemblages in a glacial fjord on King George Island: responses and implications. Ecol Indic 57: 280–292
Naeem S, Wright JP (2003) Disentangling biodiversity effects on ecosystem functioning: deriving solutions to a seemingly insurmountable problem. Ecol Lett 6:567–579
Oksanen J, Blanchet FG, Friendly M, Kindt R and others (2017) vegan: community ecology package. R package version 2.4-4. https://CRAN.R-project.org/package=vegan
Perea-Blázquez A, Davy SK, Bell JJ (2012) Estimates of particulate organic carbon flowing from the pelagic environment to the benthos through sponge assemblages. PLOS ONE 7:e29569
Pickard G (1961) Oceanographic features of inlets in the British Columbia mainland coast. J Fish Res Board Can 18:907–999
Quijon PA, Snelgrove PVR (2005) Spatial linkages between decapod planktonic and benthic adult stages in a Newfoundland fjordic system. J Mar Res 63:841–862
R Development Core Team (2013) R: a language and environment for statistical computing. R Foundation for Statistical Computing, Vienna
Richardson JR (1981) Recent brachiopods from New Zealand — background to the study cruises of 1977–79. N Z J Zool 8:133–143
Riisgård H, Larsen P (2000) Comparative ecophysiology of active zoobenthic filter feeding, essence of current knowledge. J Sea Res 44:169–193
Roddick JA (1970) Douglas Channel-Hecate Strait map-area, British Columbia. Paper No. 70-41, Geological Survey of Canada, Ottawa
Rowden AA, Schlacher TA, Williams A, Clark MR and others (2010) A test of the seamount oasis hypothesis: seamounts support higher epibenthic megafaunal biomass than adjacent slopes. Mar Ecol 31:95–106
Sebens K (1982) Competition for space: growth rate, reproductive output, and escape in size. Am Nat 120:189–197
Sebens K (1987) The ecology of indeterminate growth in animals. Annu Rev Ecol Syst 18:371–407
Smith F, Witman JD (1999) Species diversity in subtidal landscapes: maintenance by physical processes and larval recruitment. Ecology 80:51–69
Southward A, Southward E (1992) Distribution of Pogonophora (tube-worms) in British-Columbian fjords. Mar Ecol Prog Ser 82:227–233
Stone RP (2014) The ecology of deep-sea coral and sponge habitats of the central Aleutian Islands of Alaska. NOAA Prof Pap NMFS 16:1–52
Suneetha KB, Naevdal G (2001) Genetic and morphological stock structure of the pearlside, *Maurolicus muelleri* (Pisces, Sternoptychidae), among Norwegian fjords and offshore areas. Sarsia 86:191–201
Syvitski JPM, Burrell DC, Skei JM (1987) Fjords: processes and products. Springer-Verlag, New York, NY
Timothy DA, Soon MYS, Calvert SE (2003) Settling fluxes in Saanich and Jervis Inlets, British Columbia, Canada: sources and seasonal patterns. Prog Oceanogr 59:31–73
Trygonis V, Sini M (2012) photoQuad: a dedicated seabed image processing software, and a comparative error analysis of four photoquadrat methods. J Exp Mar Biol Ecol 424-425:99–108
Tunnicliffe V (1981) High species diversity and abundance of the epibenthic community in an oxygen-deficient basin. Nature 294:354–356
Tunnicliffe V, Wilson K (1988) Brachiopod populations: distribution in fjords of British Columbia (Canada) and tolerance of low oxygen concentrations. Mar Ecol Prog Ser 47:117–128
Turan C, Carvalho GR, Mork J (1998) Molecular genetic analysis of Atlanto-Scandian herring (*Clupea harengus*) populations using allozymes and mitochondrial DNA markers. J Mar Biol Assoc UK 78:269–283
Villéger S, Mason NWH, Mouillot D (2008) New multidimensional functional diversity indices for a multifaceted framework in functional ecology. Ecology 89:2290–2301
Wahl M (ed) (2009) Marine hard bottom communities: patterns, dynamics, diversity and change. Springer, Berlin
Wan D, Hannah CG, Foreman MGG, Dosso S (2017) Subtidal circulation in a deep-silled fjord: Douglas Channel, British Columbia. J Geophys Res 122:4163–4182
Webster L, Angus L, Topping G, Dalgarno EJ, Moffat CF (1997) Long-term monitoring of polycyclic aromatic hydrocarbons in mussels (*Mytilus edulis*) following the Braer oil spill. Analyst (Lond) 122:1491–1495
Wright CA, Vagle S, Hannah C, Johannessen SC, Spear D, Wan D (2016) Physical, chemical and biological oceanographic data collected in Douglas Channel and the approaches to Kitimat, October 2014-July 2015. Canadian Data Report of Hydrography and Ocean Sciences. Fisheries and Oceans Canada, Sidney
Wu Y, Hannah CG, Law B, King T, Robinson B (2016) An estimate of the sinking rate of spilled diluted bitumen in sediment laden coastal waters. In: Proc 39th AMOP technical seminar on environmental contamination and response, 7–9 June 2016, Halifax. Environment and Climate Change Canada, Ottawa, p 331–347
Yahel G, Whitney F, Reiswig HM, Eerkes-Medrano DI, Leys SP (2007) In situ feeding and metabolism of glass sponges (Hexactinellida, Porifera) studied in a deep temperate fjord with a remotely operated submersible. Limnol Oceanogr 52:428–440

Editorial responsibility: Jean-Sébastien Lauzon-Guay, Dartmouth, Nova Scotia, Canada

Submitted: July 5, 2017; Accepted: April 10, 2018
Proofs received from author(s): June 2, 2018